Electrical network model for SPRITE detectors

James A. Whitlock
Glenn D. Boreman, MEMBER SPIE
Harold K. Brown
University of Central Florida
CREOL/Electrical Engineering Department
Orlando, Florida 32816

Allen E. Plogstedt
McDonnell Douglas Missile Systems Company
701 Columbia Boulevard
Titusville, Florida 32780

Abstract. Impedance measurements were made on SPRITE (signal processing in the element) detectors. The resistive contributions were found to contain a contact resistance term, along with a term proportional to the semiconductor material length between terminals. The capacitive contributions were strongly frequency dependent and were largely independent of material length. This behavior would appear to be caused by nonohmic contacts at the metal-semiconductor interfaces where the SPRITE is bonded to its external electrical connections. When the SPRITEs were illuminated, the resistance decreased as expected, but the capacitance showed a sizable increase as well. A *T*-network model is developed that is consistent with the set of two-terminal impedance measurements. A model of this type should provide a useful starting point for electronics optimizations in SPRITE systems, including the design of the bias source, the readout mechanism, and the preamplifier.

Subject terms: infrared imaging systems; detectors; signal processing.

Optical Engineering 30(11), 1784–1787 (November 1991).

CONTENTS

1. Introduction
2. Measurement setup
3. Measurement results
4. Conclusion
5. Acknowledgments
6. References

1. INTRODUCTION

A SPRITE (signal processing in the element)[1] detector, shown in Fig. 1, is a three-terminal photoconductive device. Each SPRITE has a "bias" terminal at the left of the figure. The "return" terminals are at the center of each detector, at the right-hand side of the figure. The "output" terminal for each detector is connected at the beginning of the tapered readout region. The advantage of SPRITE detectors is that a time-delay-and-integration[2] (TDI) operation is performed as follows, without the need of an external delay line. A dc voltage is established across the bias and return terminals, which causes any photogenerated carriers to drift toward the return terminal. When the (diffusion-limited) charge packet associated with a particular image feature drifts past the output terminal, a voltage change is produced across the output-to-return terminals that is proportional to the number of photogenerated carriers in that packet. The infrared image falling on the SPRITE is mechanically scanned at a velocity equal to the drift velocity of the carriers. This increases the signal-to-noise ratio of the detected image by effectively increasing the dwell time of the detector on any particular image feature. The signal grows with the dwell time, whereas the noise, being uncorrelated, grows as the square root of the dwell time.

There has been considerable recent research on optimization of SPRITE parameters, including bias voltage,[3] bar length,[4] readout geometry,[5,6] bar geometry,[7,8] and anamorphic ratio in the optics.[9,10] Similar optimization of preamplifier designs, bias circuitry, and readout mechanisms would be facilitated if designers had an accurate network model for SPRITEs. The impedance measurements presented herein were performed as a function of frequency, bar length, and illumination level, and have led to the development of such a network model.

Investigation of the frequency dependence of impedance is of interest because the SPRITE operates over a range of electrical frequencies[11] of approximately 100 Hz to 600 kHz, which are related to the image-plane spatial frequencies by the carrier drift velocity.

2. MEASUREMENT SETUP

The actual SPRITE detectors measured are those seen in Fig. 1 and had total lengths between 450 and 650 μm, with exponentially tapered[5,6] readout regions 50 μm long. These SPRITEs were fabricated on *n*-type HgCdTe, optimized for use in the 3- to 5-μm band of wavelengths. The detectors were held at 190 K in a vacuum dewar.

Impedance measurements were made with a Hewlett-Packard 4192 impedance analyzer. This instrument provided a sinusoidal test voltage of adjustable amplitude, at a specified frequency, between any two terminals of the SPRITE. An ac current response was measured, from which the complex impedance was calculated. For each measurement, impedance data was available from the instrument as a parallel combination of resistance and capacitance values, or as magnitude and phase of complex impedance seen across that terminal pair. A dc bias of 2 V across bias to return was supplied by an external battery source, so that the SPRITE would be operating under dc bias conditions.

The test voltages used were intended to electrically simulate the signals that the SPRITE produces under normal illumination conditions, which are in the range of tens of microvolts. The actual test voltage amplitude for our measurements was 10 mV,

Invited paper IR-016 received April 19, 1991; revised manuscript received July 9, 1991; accepted for publication July 10, 1991.

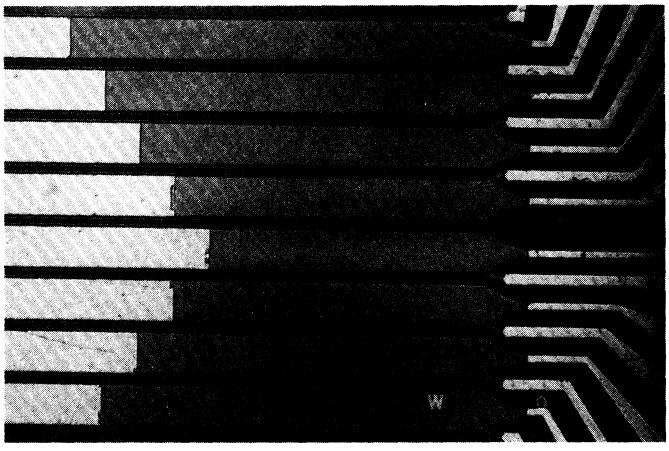

Fig. 1. Actual SPRITE detectors tested. The shortest bar is 450 μm, the longest is 650 μm. All SPRITEs had horn-shaped readouts.

which was the smallest amplitude that gave accurate impedance results using the HP4192.

In some measurements, the SPRITE detectors were flood illuminated with radiation from a 500 K blackbody, to investigate the dependence of impedance on flux level. The received flux level was controlled with an aperture wheel.

In all cases, the measured SPRITE impedance was corrected for the impedance of the power supplies (from the battery for dc and from the impedance analyzer instrument for ac) as well as for the capacitance of the external detector wires. This calibration was carried out using a dummy load resistor of known characteristics. Measurements on this load provided a base-line impedance that was subtracted from the measured data.

3. MEASUREMENT RESULTS

The first electrical parameter considered is resistance, which has a contribution proportional to the length of the semiconductor material across which the measurement is made, consistent with the usual expression for resistance,

$$R = \rho L/A \ , \qquad (1)$$

where ρ is the resistivity, L is the material length, and A is the cross-sectional area. We show results of bias-to-return resistance measurements in Fig. 2 for SPRITE lengths of 450, 500, 600, and 650 μm. At frequencies above 100 kHz, the results for the bars are 1690, 1850, 2040, and 2140 Ω, respectively. A linear fit to the R versus L data yields a contact resistance value (for $L=0$) of approximately 650 Ω. With that value subtracted, a resistance per unit length of these SPRITEs is obtained as 2.3 Ω/μm for all bars. Below 100 kHz, we measured approximately a 3% increase in resistance in going to zero frequency, which might be caused by either contact effects or the SPRITE geometry.

When the SPRITE detectors were flood illuminated by a 500 K blackbody source, the resistance dropped as expected for a photoconductive device. The resistance decrease seen was 0.58% for a 0.6-μW input and 9.8% for a 15-μW input. This effect was not frequency dependent, keeping the same curve shapes seen in Fig. 2.

We then measured the capacitance of the SPRITEs as a function of frequency, with results shown in Fig. 3 for bias-to-output, in Fig. 4 for output-to-return, and in Fig. 5 for bias-to-return

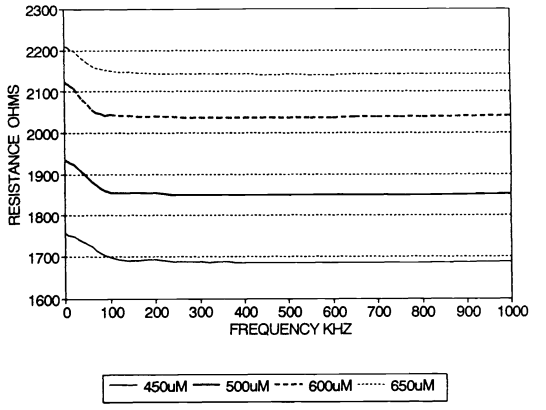

Fig. 2. Bias-to-return resistance versus frequency curves, parametrized on SPRITE length.

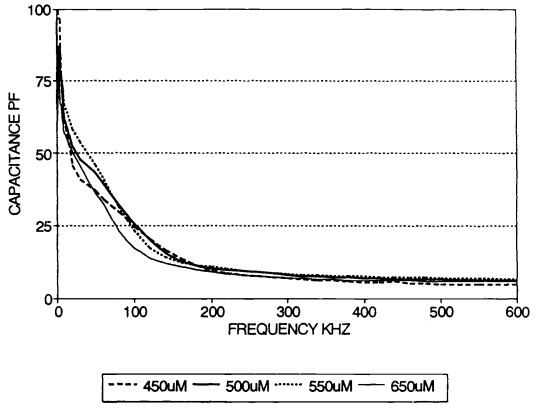

Fig. 3. Bias-to-output capacitance versus frequency curves, parametrized on SPRITE length.

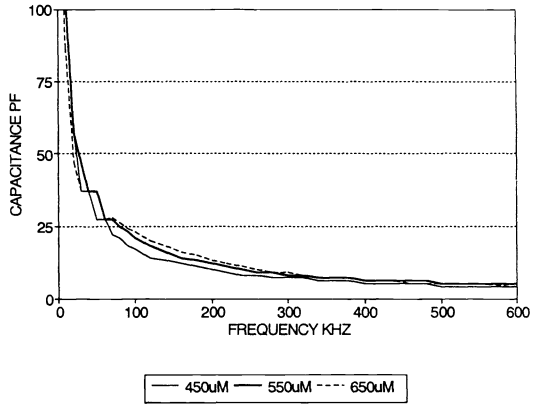

Fig. 4. Output-to-return capacitance versus frequency curves, parametrized on SPRITE length.

terminal pairs. All of these measurements were made with a bias-to-return voltage of 2 V. Comparing the two sets of curves that have material length as a parameter (Figs. 3 and 4), the main feature noted is that although the material distance between terminals for the data in Fig. 3 is in the range of 400 to 600 μm and the material distance between terminals for the data in Fig. 4 is 50 μm, the capacitance values on both sets of curves are nearly the same. This indicates that the main contribution to capacitance of the SPRITE devices is a junction capacitance that is independent of the length of the structure. Indeed, a previously

published non-quasi-static model[12] of space-charge-region capacitance for metal-semiconductor junctions predicts a decreasing junction capacitance with increasing frequency. The dependence of capacitance on the SPRITE length shows up as smaller variations (in the range of a few percent to ≈20%) in the curves of Figs. 3 and 4. A theoretical basis for these variations is difficult to identify from the data (and may in fact be due to differences in contacts on the individual detectors), but the magnitude and main features of the curves should be useful information for initial optimizations of SPRITE electronics designs.

Figure 5 shows the bias-to-return capacitance as a function of frequency (for a 650-μm SPRITE), with illumination levels of 0, 0.6, and 15 μW from the 500 K blackbody. For the 15-μW flux level, the capacitance increases by approximately a factor of 2 for frequencies below 400 kHz. This behavior is probably attributable to the characteristics of the metal-semiconductor junctions under the bias conditions seen under illumination.

The convenient use of these types of measurements for SPRITE electronics optimization requires the incorporation of the measured data into an appropriate model. Taking a simple T-model network, as seen in Fig. 6, to represent the SPRITE, we can solve for the model's impedance values Z_1, Z_2, and Z_3 in terms of the measured two-terminal impedances Z_{br}, Z_{bo}, and Z_{or}. The relationships are

$$Z_1 = \frac{Z_{bo} - Z_{or} + Z_{br}}{2}; \qquad Z_2 = \frac{Z_{br} - Z_{bo} + Z_{or}}{2};$$

$$Z_3 = \frac{Z_{or} - Z_{br} + Z_{bo}}{2}, \tag{2}$$

where each of the terms will be frequency dependent because of the metal-semiconductor junctions. Such a T network, based on measured data for representative SPRITE detectors of a given material composition and geometry, would provide a useful starting point for design optimizations of the bias source, readout configuration, and preamplifier.

4. CONCLUSION

Impedance measurements on 3- to 5-μm band SPRITE detectors indicate that the resistance includes a term for contact resistance along with a term that is linear with material length. Capacitance effects are strongly frequency dependent, with increasing capacitance at low frequencies. SPRITE capacitance also increases with illumination level. Capacitance appears to be mainly caused by the metal-semiconductor junctions, since the capacitance is seen to be almost independent of material length. A simple T network having three impedances can be developed from data measured across the bias-to-return, bias-to-output, and output-to-return terminals.

Even without a detailed investigation of the physics involved in the specific junction behavior observed, we hope that this measurement and modeling approach will be a useful starting place for optimization of SPRITE electronics for the bias source, the readout mechanism, and the preamplifier.

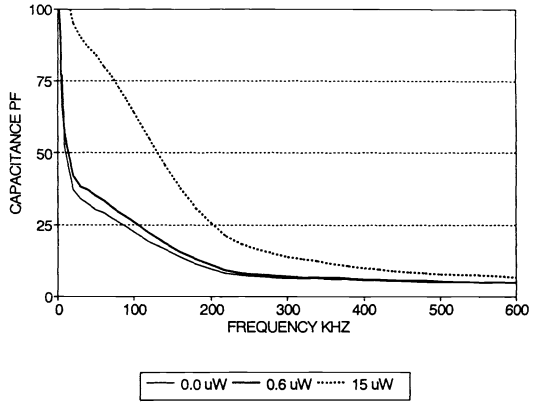

Fig. 5. Bias-to-return capacitance versus frequency curves, parametrized on received flux level, for a 650-μm SPRITE length.

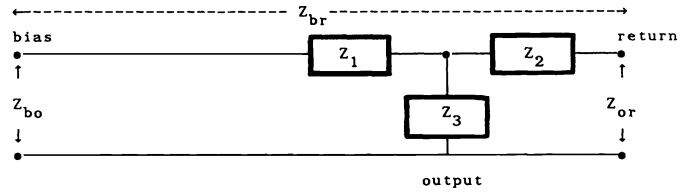

Fig. 6. *T*-network model for SPRITE, where Z_1, Z_2, and Z_3 are model impedances and Z_{bo}, Z_{br}, and Z_{or} are measured two-terminal impedances from bias to output, bias to return, and output to return, respectively.

5. ACKNOWLEDGMENTS

This work was supported by McDonnell Douglas Missile Systems Company and by the Florida High Technology and Industry Council. It was reviewed by the Department of Defense Directorate for Freedom of Information and Security Review (DFOISR) and is approved for public release; distribution is unlimited. Case No. 90-0987.

6. REFERENCES

1. C. T. Elliott, "New detector for thermal imaging systems," *Electron. Lett.* 17, 312–313 (1981).
2. J. M. Lloyd, *Thermal Imaging Systems*, pp. 331–335, Plenum Press, New York (1975).
3. G. V. Poropat, "The effect of bias voltage on SPRITE detector MTF," *Infrared Phys.* 26, 9–15 (1986).
4. G. D. Boreman and A. E. Plogstedt, "MTF and number of equivalent elements for SPRITE detectors," *Appl. Opt.* 27, 4331–4335 (1988).
5. T. Ashley, C. T. Elliott, A. M. White, J. Wotherspoon, and M. D. Johns, "Optimization of spatial resolution in SPRITE detectors," *Infrared Phys.* 24, 25–33 (1984).
6. G. D. Boreman and A. E. Plogstedt, "Spatial filtering by a line-scanned nonrectangular detector: Application to SPRITE readout MTF," *Appl. Opt.* 28, 1165–1168 (1989).
7. J. Wotherspoon, R. J. Dean, M. D. Johns, T. Ashley, C. T. Elliott, and A. M. White, "Developments in SPRITE infrared detectors," in *Infrared Technology X*, Proc. SPIE 510, 102–112 (1984).
8. X. Zhijun and F. Wenqing, "Optimization of SPRITE detectors," *Infrared Phys.* 30, 489–497 (1990).
9. A. Campbell, C. T. Elliott, and A. M. White, "Optimization of SPRITE detectors in anamorphic imaging systems," in *Advanced Infrared Detectors and Systems*, IEE Conference Publication 263, 18–23 (1986).
10. P. Fredin, "Optimum choice of boost filter parameters and anamorphic ratio for a SPRITE-based IR sensor," in *Infrared Imaging Systems: Design, Analysis and Testing II*, G. Holst, ed., Proc. SPIE 1488, 432–442 (1991).
11. K. Barnard, G. Boreman, A. Plogstedt, and B. Anderson, "MTF measurement of SPRITE detectors: Sine wave response," *Appl. Opt.* 30(31) (1991).
12. J. J. Liou and D. C. Malocha, "Modeling the non-quasi-static metal-semiconductor space-charge-region capacitance," *J. Appl. Phys.* 65, 1782–1787 (1989).

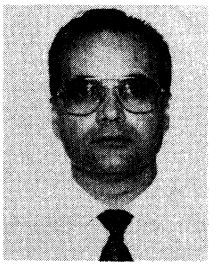

James A. Whitlock received his BA degree in English from Marquette University in Milwaukee, Wisconsin, in 1969, and BS and MS degrees in electrical engineering from University of Central Florida in 1988 and 1991, respectively. He was a graduate research assistant in the Infrared Systems Laboratory at University of Central Florida/CREOL. He is now employed as an electrical engineer, attached to the Naval Sea Combat Systems Engineering Station, Norfolk, Virginia.

Glenn D. Boreman: Biography and photograph appear with the paper "Modulation transfer function characterization and modeling of a Scophony infrared scene projector" in this issue.

Harold K. Brown received his BS degree in electrical engineering from Florida Institute of Technology in 1975, and MS and Ph.D. degrees in electrical engineering from Ohio State University in 1977 and 1980, respectively. He then joined the DRAM development group at Intel Corporation working on the 64K and 1Mbit technologies. He is presently on a joint appointment with University of Central Florida and Florida Institute of Technology researching the design and test of integrated circuits for high-performance imaging and computing. Dr. Brown is a member of IEEE.

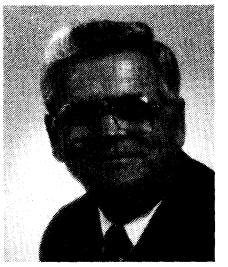

Allen E. Plogstedt received his BS and MS degrees in electrical engineering from the University of Cincinnati in 1956 and 1965, respectively. He joined Avco Electronics in Cincinnati in 1956. In 1967, he moved to McDonnell Douglas Missile Systems Company in Titusville, Florida, where he is currently staff director of Engineering. Plogstedt is a McDonnell Douglas Fellow and holds four patents. He is a member of IEEE, AIAA, ADPA, and AUSA.